

# We are IntechOpen, the world's leading publisher of Open Access books Built by scientists, for scientists

6,900

Open access books available

185,000

International authors and editors

200M

Downloads

Our authors are among the

154

Countries delivered to

TOP 1%

most cited scientists

12.2%

Contributors from top 500 universities



WEB OF SCIENCE™

Selection of our books indexed in the Book Citation Index  
in Web of Science™ Core Collection (BKCI)

Interested in publishing with us?  
Contact [book.department@intechopen.com](mailto:book.department@intechopen.com)

Numbers displayed above are based on latest data collected.  
For more information visit [www.intechopen.com](http://www.intechopen.com)



# The Microstructure Characterization and the Mechanical Properties of Electrospun Polyacrylonitrile-Based Nanofibers

Chen Zhang, Xuejia Ding and Sizhu Wu

*Key Laboratory of carbon fiber and functional polymers, Ministry of Education,  
College of Materials Science & Engineering, Beijing University of Chemical Technology,  
Beijing,  
China*

## 1. Introduction

Electrospinning provides a straightforward and cost-effective approach to produce fibers from polymer solutions or melts having the diameters ranging from sub-microns to nanometers (Reneker & Chun 1996 ; Dzenis 2004; Hammel et al. 2004; Greine & Wendorff 2007). The nanofiber fabrication by the electrospinning technique can also provides high orientation of the polymer chains by some special collecting accessories due to the high elongation forces that developed during the electrospinning process. This process is accompanied by massive solvent evaporation which leads to fibers with high packaging density(Doshi & Reneker 1995). The carbon fibers possess high mechanical strengths and moduli, superior stiffness, excellent thermal and electrical conductivities, as well as strong fatigue and corrosion resistance; therefore carbon nanofibers have recently received increased attention for their potential applications as composite reinforcing fillers, heat-management materials, high-temperature catalysts, membrane-based separation media, and components in nanoelectronics and photonics etc.(Chand 2000). There are several precursors for the production of carbon fiber, such as polyacrylonitrile (PAN), pitch and cellulose(Edie 1998; Basova et al. 2004) etc. But PAN is the most widely used precursor for manufacturing high-performance fibers due to its combination of tensile and compressive properties as well as its high carbon yield(Sutasinpromprae et al. 2006). Usually, the PAN or PAN-based carbon fiber is produced by the following steps: (1) first, spinning the precursor under different drawing ratio, (2) then, the precursor fiber is stabilized at 200 to ca. 300°C in an oxidation atmosphere; (3) finally, the stabilized fiber is heated at temperatures from 1200 to ca. 3000 °C in an inert atmosphere to wipe off nearly all of the non-carbon element to obtain the final carbon fibers. There are two critical factors in these manufacturing processes of PAN carbon fibers which one is to control the suitable orientation and crystallization of the precursors and the other is the post-treatment steps such as pre-oxidization, stabilization and carbonization. Conventional PAN-based carbon fibers typically have diameters ranging from 5 to 10  $\mu\text{m}$  (Morgan 2005). However, the electrospun PAN nanofibers are uniform with the diameters of approximately 300 nm (Chun et al. 1999; MacDiarmid et al. 2001), which is more than 30 times smaller than their conventional counterparts. The high specific surface

area of electrospun polymer and carbon nanofibers leads to the enhanced properties in various applications such as electrodes in fuel cells and supercapacitors. The subsequent thermal treatments, including pre-oxidization, stabilization and carbonization, convert the PAN precursor nanofibers into carbon nanofibers that are very long (continuous) probably with desired microstructural, electrical, mechanical, and other properties. However, the mechanical properties of electrospun nanofibers need to be improved because of the limited crystallinity and orientation during the electrospinning (Li et al. 2003). The microstructures and the related mechanical and/or electrical properties of the electrospun carbon nanofibers are still largely unknown.

Carbon nanotubes (CNTs) have achieved a momentous research and application interest due to their unique properties, such as high tensile modulus, good heat and electrical conduction, unique optical and electronic properties, and so forth. It is found that reinforcement of polymers by CNTs may significantly improve their mechanical properties, thermal stability, electric conductivity, and other functional properties. For enhancing the properties of the nanofibers, the carbon nanotubes (CNTs) have also tried to introduce in the PAN-based composites due to their appealing mechanical (Wong et al. 1997; Yu et al. 2000), electrical (Javey et al. 2003), and thermal conductivity properties (Miaudet et al. 2007). Both single-walled carbon nanotubes (SWNTs) and multiwalled carbon nanotubes (MWNTs) are of scientific interest in nanotechnology and nanodevices because of their superior structural, mechanical, chemical, thermal, and electrical performance (Iijima 1991; Baughman et al. 2002; Collins et al. 2001). The SWNT reinforced pitch-based carbon microfibers (Andrews et al. 1999) and PAN/CNTs microfibers (Sreekumar et al. 2004) exhibited a significant improvement in mechanical properties and thermal stability. It has been shown that significant interactions exist between PAN chains and CNTs, which lead to higher orientation of PAN chains during the heating process (Rilutsky et al. 2010). It is also shown that CNTs embeds in electrospun PAN nanofiber serve as nucleation centers for graphitic structure formation during the carbonization process leading to a more ordered and oriented structure. For pre-oxidization, stabilization and carbonization, it is noteworthy that applying tension during thermal treatments, particularly during stabilization, is crucial for the development of carbon fibers with high mechanical strength; i.e., if the stabilization is carried out without tension, the resulting carbon fibers are mechanically weak (Donnet et al. 1998; Morgan 2005). However, before full realization of their reinforcing improvement, the following two crucial issues have to be solved: (i) dispersion and orientation of CNTs in the nanofiber (Chandrasekar et al. 2009; Hao et al. 2006), good interfacial bonding is required to achieve load transfer across the CNTs-matrix interface (Chen et al. 2006); (ii) the macroscopic alignment in the nanofibers (Na et al. 2009) and the orientation and crystallinity of polymer chains. Therefore, in this chapter, the manufacturing process and characterization methods for the microstructures and mechanical properties of PAN and PAN-based nanofibers has been reviewed.

## **2. Manufacturing and characterization of the PAN and CNTs/PAN composites nanofibers**

### **2.1 Manufacturing of the PAN and PAN-based nanofibers**

The PAN and PAN-based nanofibers can be made by electrospinning with the nominal electric field on the order of 1 kV/cm. Fig.1 is the schematic diagram of the electrospinning technique. In the process the PAN or CNTs/PAN solution is held by its surface tension at

the end of a capillary, such as a stainless steel needle. As the intensity of the electric field is increased, usually by increasing the voltage, the hemispherical surface of the solution at the tip of the capillary tube elongates to form a structure named as a Taylor cone (Taylor 1969). At a certain voltage the electrical forces overcome the surface tension and a jet ejects from the Taylor cone. The jet travels some distance and then a whipping instability begins to further attenuate the jet into nanofibers. The fibers are collected onto a counter electrode, such as a screen, drum, plate, or the edge of a rotating disk. Coupled with the usual observations the fact that fibers can be electrospun using an Ac field indicates that a portion of the attenuation occurs in the stable jet region. The Dc electrospun fibers are smaller than Ac spun fibers indicates further drawing occurs in the instability region. The voltage between the electrode and the counter electrode could be controlled by the high voltage power supply such as setting at 14-16 kV. The collector rotated at some surface speed such as 6.6m/s, which the high speed rotating collector could align the nanofibers into the nanofiber sheets.

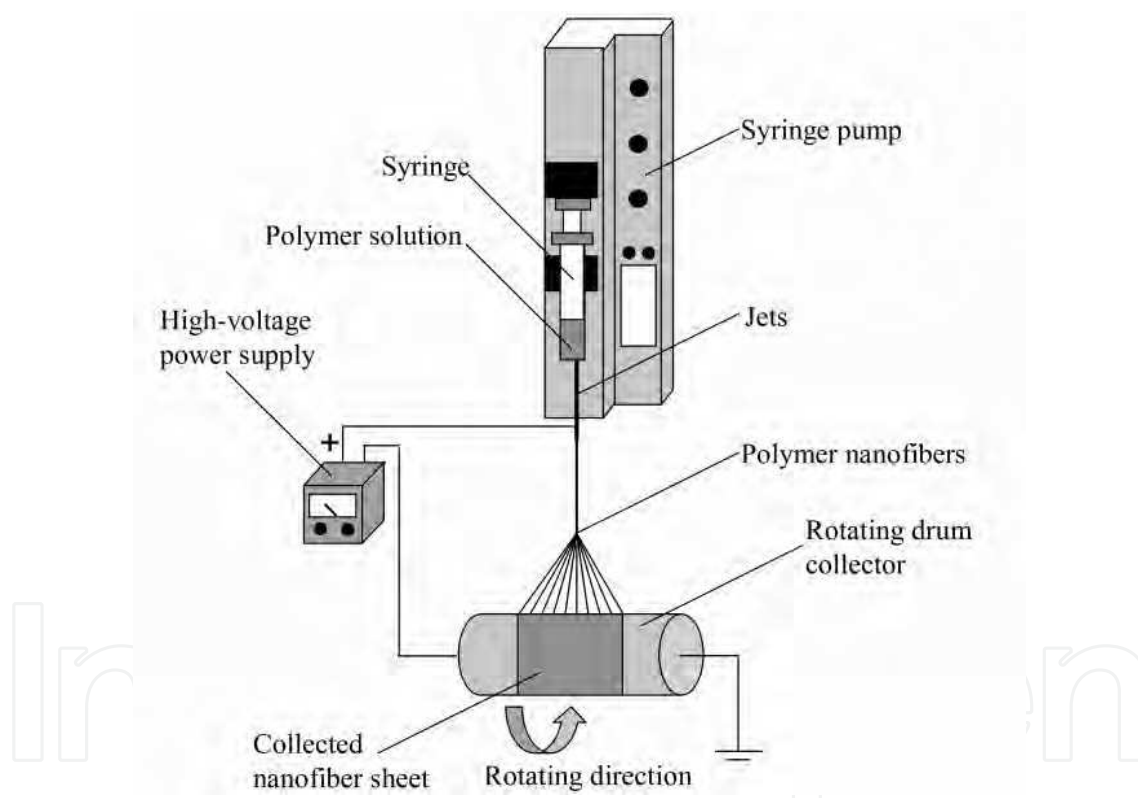


Fig. 1. Schematic diagram of the electrospinning technique.

Since N,N-dimethylformamide(DMF) is the common solvent of PAN-based carbon fibers manufacturing process which can easily evaporate during the electrospinning, the DMF can be selected as solvent and are through mild bath sonication to have a completely dissolution. Usually the suitable weight concentration of PAN/DMF can be selected higher than 10% with the PAN average molecular weight of 100,000 g/mol. Fig. 2 shows the SEM micrographs of different concentrations of electrospinning PAN/DMF solutions of 8 wt %, 10 wt % and 12 wt % respectively. At the 8 wt% PAN/DMF ratio (Fig. 2A), viscous forces

within the jet are insufficient to stabilize disturbances, leading to capillary breakup. At 10 wt% and 12 wt% PAN/DMF ratios, irregular and regular beads formed, respectively (Fig. 2B,C). Therefore it can be said as the PAN/DMF ratio increases higher than 10wt%, viscous forces stabilize disturbances at the jet surface, leading to a beads-on-string configuration. However, if the concentration was too high, controlling and maintaining a stable flow rate becomes very difficult because the viscosity of the polymer solution is high.

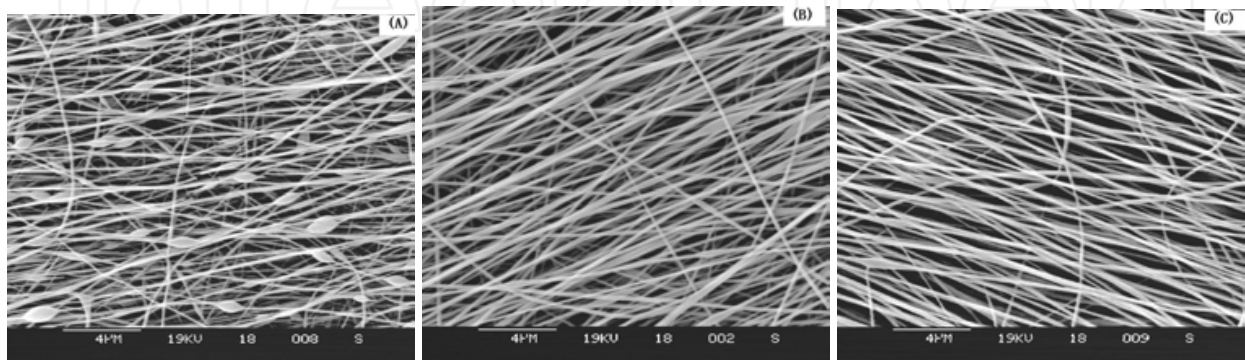


Fig. 2. SEM micrographs of PAN/DMF different concentrations of electrospinning nanofibers with the solutions of (A) 8 wt %; (B) 10 wt %; (C) 12 wt %.

To uniformly disperse the CNTs in the organic polymer matrix, the CNTs are modified to form an individually polymer-wrapped structure (Waclawik et al. 2006). As is well known, polymer wrapped greatly inhibits the Van der Waals attraction between the polymer with solvent and the interactional polymer chains which normally observed between separate SWNTs with small ropes of SWNTs, such as the SWNTs can be wrapped by regioregular poly(3-hexyl thiophene) (rrP3HT). These effects caused the wrapped nanotubes to be much more readily suspended in concentrated SWNTs solutions and suspensions, which in turn substantially enabled manipulation of SWNTs into various bulk materials, including films, fibers, solids, and composites of all kinds (Smalley et al. 2007).

For example, a 0.75 wt% SWNTs based PAN composite solution is prepared as follows; (1) first, a given weight of SWNTs is first dispersed for 2 h in DMF through mild bath sonication, which is followed by the addition of PAN (128.91 mg per milliliter of SWNTs/DMF solution); (2) then, the mixture is mechanically stirred overnight at 40 °C using a magnetic stirrer to yield a homogeneous solution. Fig. 3 SEM shows the micrographs of PAN and PAN/SWNTs nanofibers by electrospinning with different SWNTs concentrations.

The relatively aligned PAN nanofibers and PAN/SWNTs composite nanofibers can be obtained by electrospinning by the set-up of a rotating instrument. Thus, for collection of the large area aligned nanofibers, a parallel rotating drum can be adopted. Such as in our study, the 0.16 m perimeter collector rotated at a surface speed about 6.6 m/s, that the high speed rotating collector could align the nanofibers into the nanofiber sheets. Fig. 4 shows the schematic diagram of the frame to prepare the aligned nanofibers films with (a) the 16cm×12cm paper frame with the hollow of 16cm×4cm wrapping around (b) the rotating drum and (c) the sheet after electrospinning. And the SEM photographs of different speeds of rotation are shown in Fig. 5, which indicates the higher rotating speed leads to higher alignment of the nanofibers.



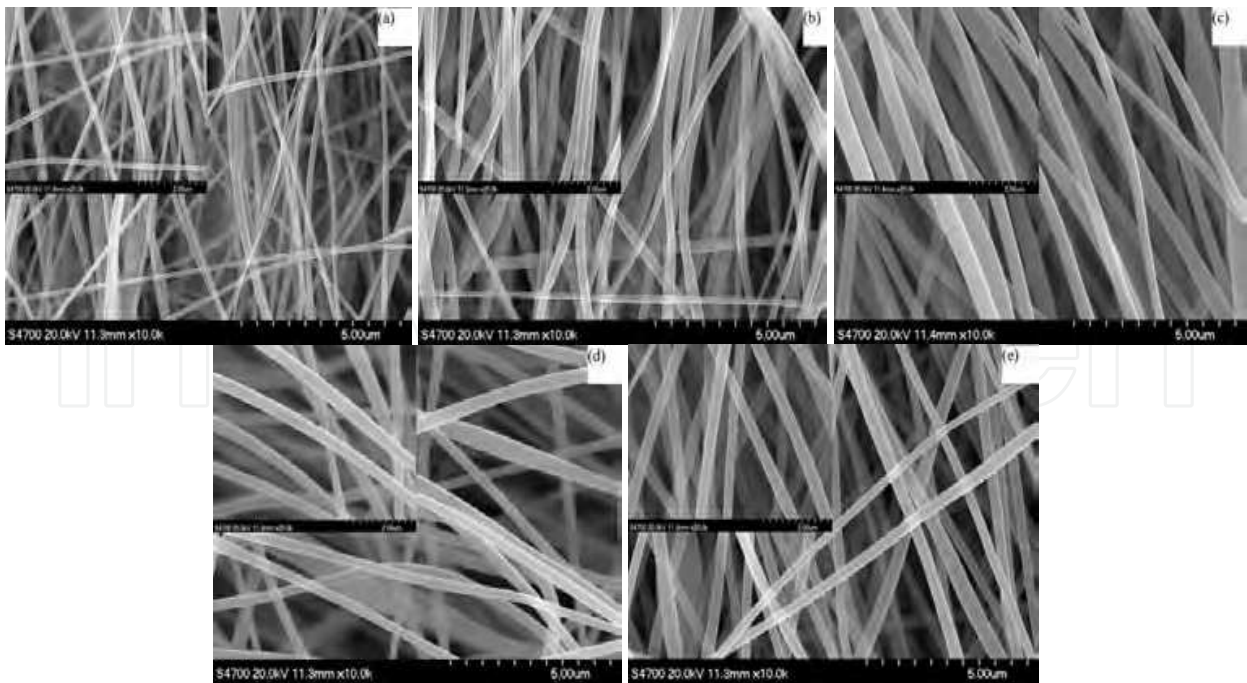


Fig. 3. SEM micrographs of PAN and PAN/SWNTs nanofibers with different SWNTs concentration (a)0wt% (b)0.25wt% (c)0.5wt% (d)0.75wt% (e)1wt%.

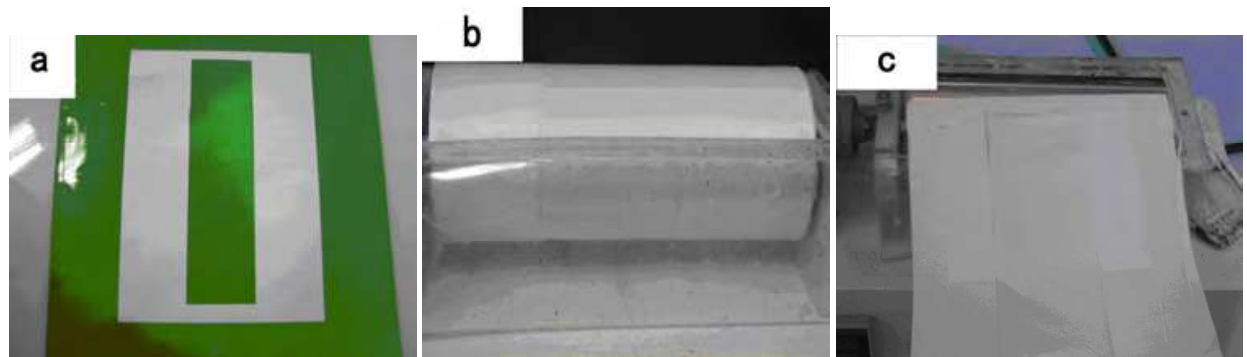


Fig. 4. Schematic diagram of the frame to prepare the aligned nanofibers films (a) the 16cm×12cm paper frame with the hollow of 16cm×4cm (b) on the rotating drum (c) after electrospinning.

During the electrospinning process, however, the whirlpool jet from the pinhead to the collector still made it difficult to get the unidirectional alignment in a large-area sheet (Huang et al. 2003), making the subsequent hot-stretched procedure particularly useful, which is also the key process during the manufacturing of carbon fibers. Therefore, the electrospun nanofibers needed a subsequent hot-stretch to improve the fiber alignment. The PAN nanofibers and PAN/SWNTs composite nanofibers can be hot-stretched according to the method proposed by Phillip and Johnson (Johnson 1965; 1966). Some methods have been tried, such as the both ends of the nanofiber sheet (size of 4 cm width × 10 cm length with 17 μm thickness) can be clamped with the pieces of graphite plates. Then, one end was fixed to the ceiling of the oven and the other end can be weighted by some of metal poise (75g) to give a desired tension and elongation in the temperature-controlled oven at 135 ± 2°C for 5 min. The schematic diagram of hot-stretching of nanofiber sheet is shown in Fig. 6.

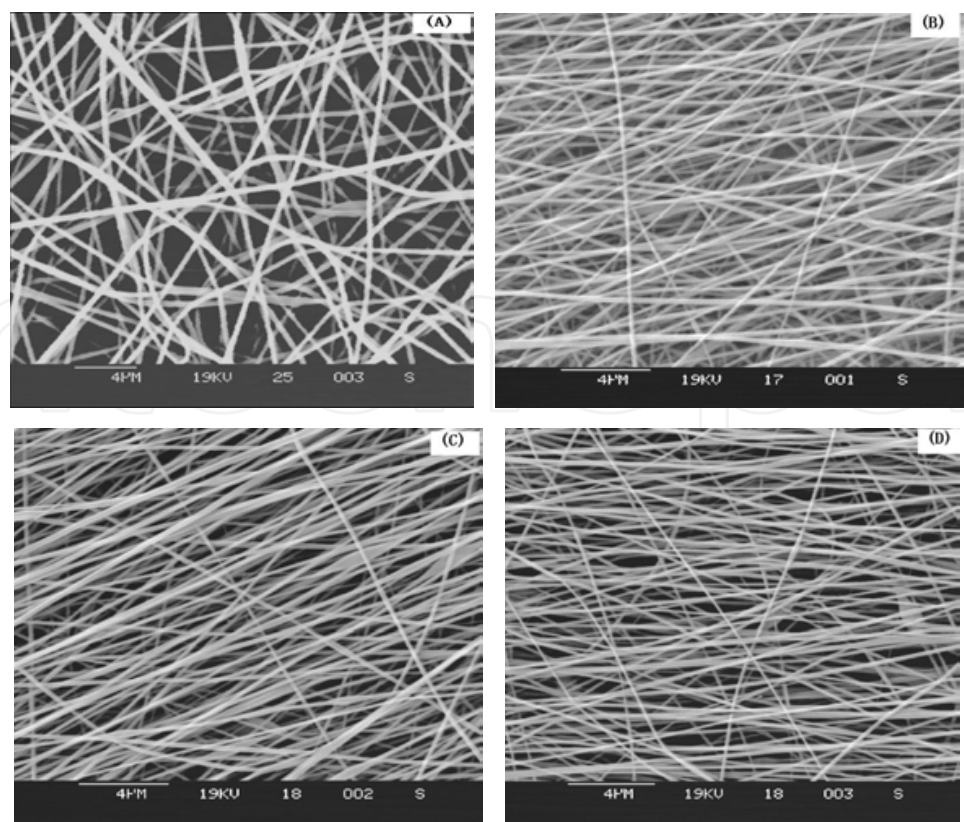


Fig. 5. SEM photographs of different speed of rotation (a) non-woven fabrics, (b) 6.28 m/s, (c) 10.47 m/s, and(d) 14.65m/s.

The stretching ratio,  $\lambda$ , can be calculated from  $\lambda = L/L_0$ , where  $L$  and  $L_0$  are the lengths of nanofiber sheet after and before the hot-stretching, respectively. Fig. 7 is the SEM micrographs of as-spun and hot-stretched PAN nanofibers, and the cross sectional views of as-spun and hot-stretched one respectively. It can be seen that the high alignment and density can be achieved by hot-stretched process.

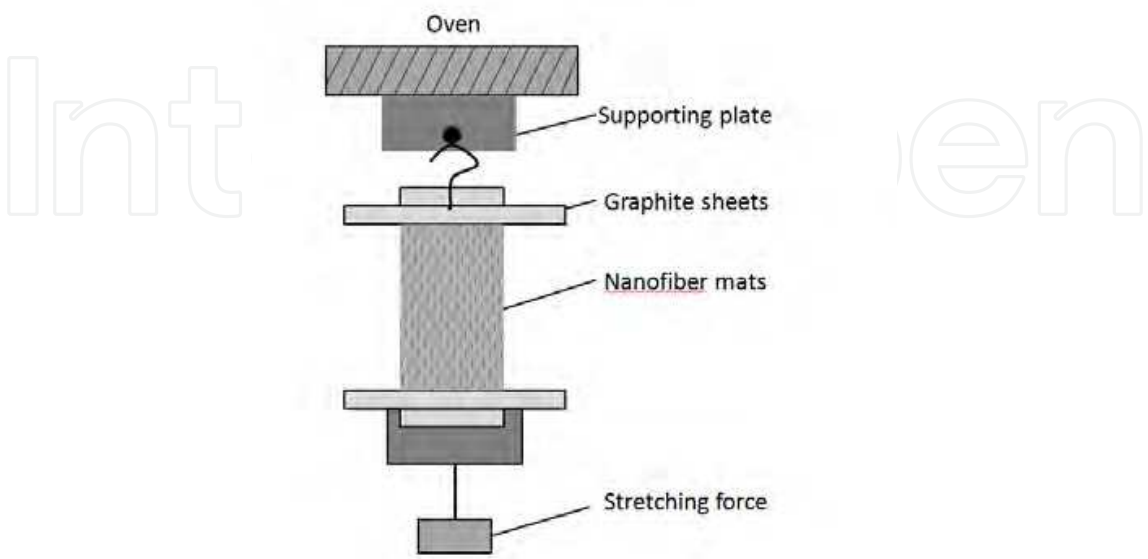


Fig. 6. The schematic representation of the experimental setup for hot-stretching process.

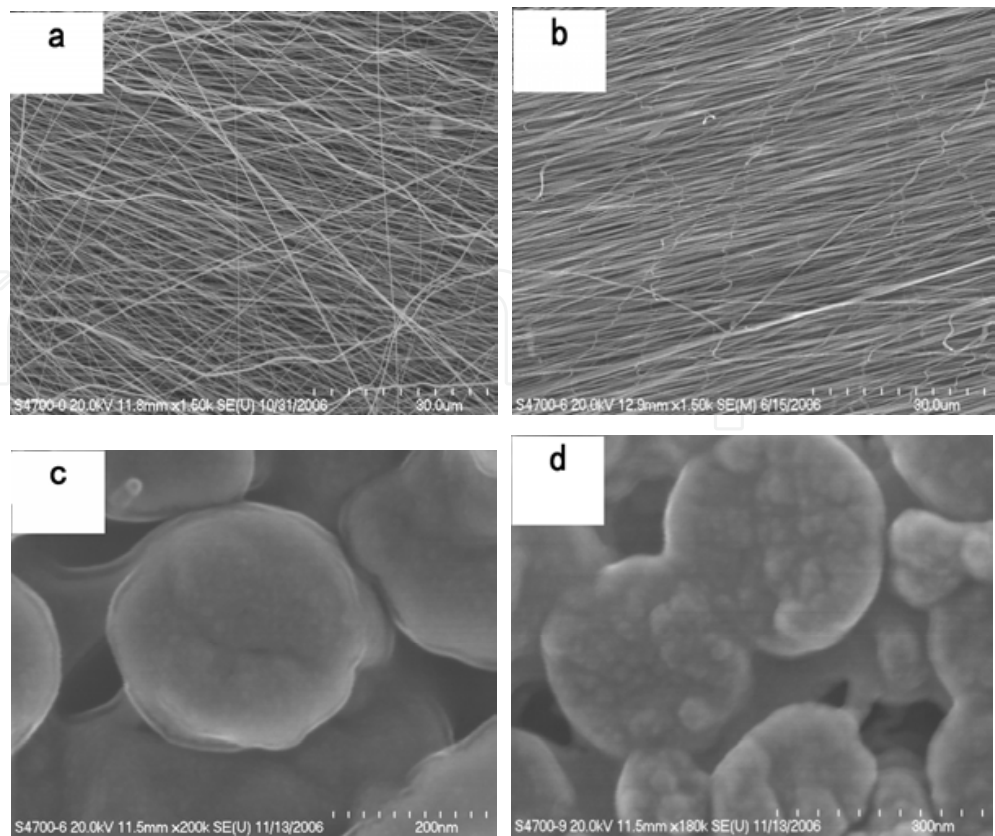


Fig. 7. SEM micrographs: (a) as-spun nanofibers, (b) hot-stretched nanofibers, (c) cross sectional views of as-spun nanofibers and (d) hot-stretched nanofibers.

2.2 Characterization of microstructures and mechanical properties

2.2.1 Morphology of PAN and PAN-based composite nanofibers

The optical micrograph (OM) images of electrospinning composites nanofibers mats are shown in Fig. 8 which the color becomes dark consequently. This is due to the different concentrations of the CNTs. Since the cross-sectional area of spinning nanofibers is very small, these nanofibers can be potentially used as optics transparency materials such as the optical filter etc.



Fig. 8. OM images of PAN and PAN/SWNTs nanofibers using (a)0wt% (b)0.25wt% (c)0.5wt% (d)0.75wt% (e)1wt% SWNTs concentrations.

The diameters of the PAN nanofibers which are directly electrospun on a TEM-copper-grid can be observed by scanning electron microscopy (SEM), which the diameters of electrospun nanofibers can be analyzed with image analyzer software (Image J). The results of the diameter distribution of PAN and PAN/SWNTs nanofibers with different SWNTs concentration 0wt%, 0.25wt%, 0.5wt%, 0.75wt% and 1wt% are shown in Fig. 9. The diameter locates between 100 to 500nm which is just the range of nano-scale.



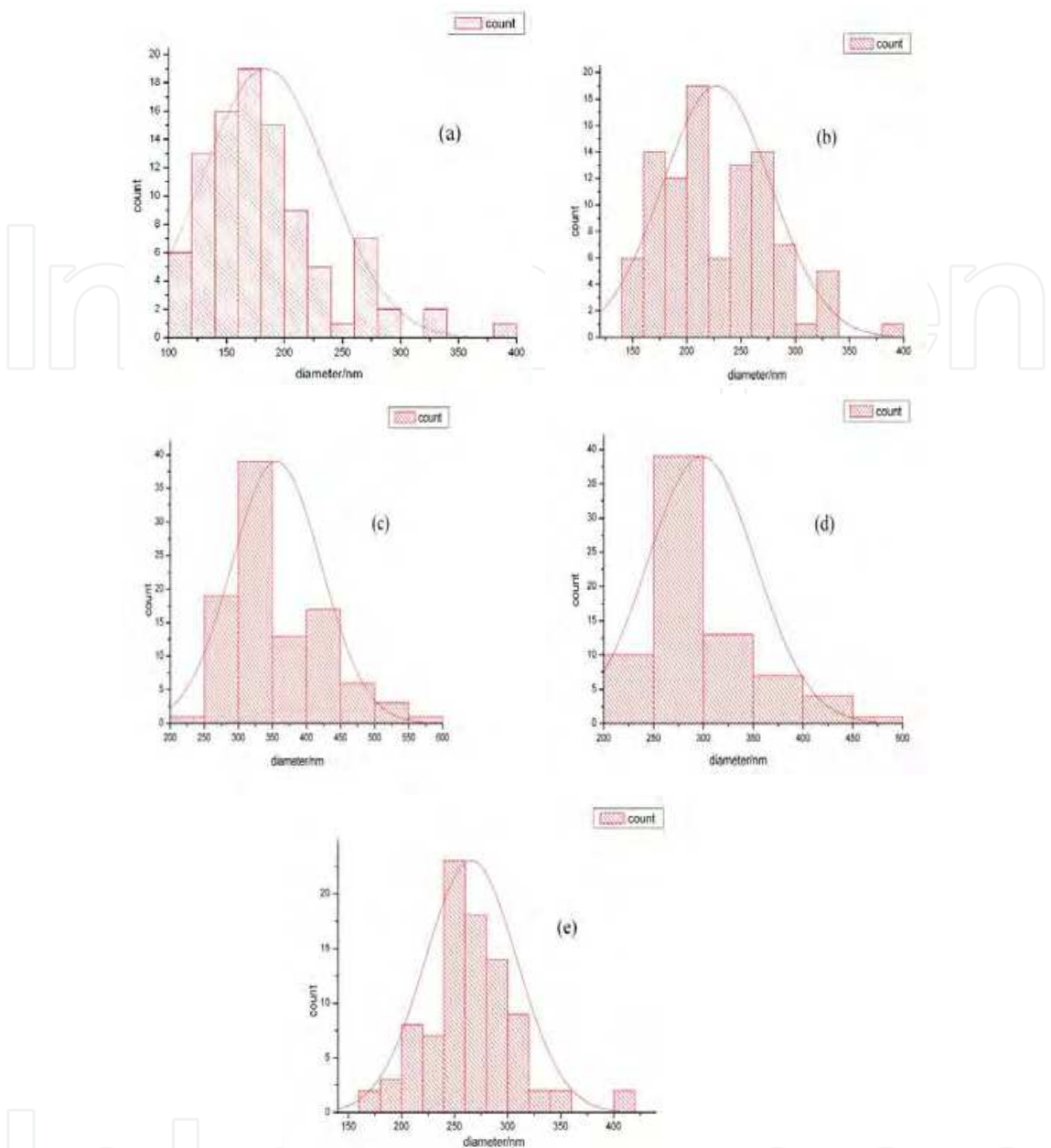


Fig. 9. The diameter distribution of PAN and PAN/SWNTs nanofibers with different SWNTs concentration (a)0wt% (b)0.25wt% (c)0.5wt% (d)0.75wt% (e)1wt%.

Fig. 10 compares the SEM micrographs of as-spun and hot-stretched PAN nanofibers and as-spun PAN/SWNTs composite nanofibers. It can be seen that there is no obvious conglutination in the nanofibers after the introduction of SWNTs. And Fig. 10(c) shows the hot-stretched PAN nanofibers, documenting the good alignment along the sheet axis after the hot-stretched process. It can further be found that the alignment of the fibers became closer to parallel after being hot-stretched. Also, the average diameters of the original as-spun fibers are significantly reduced from 200 nm to 120 nm after hot-stretching. In order to demonstrate that the prepared nanofibers do contain some oriented SWNTs, transmission electron microscopy (TEM) can be utilized to view the alignment and orientation of SWNTs within the nanofibers manufacturing process. As seen by TEM in Fig. 11, the

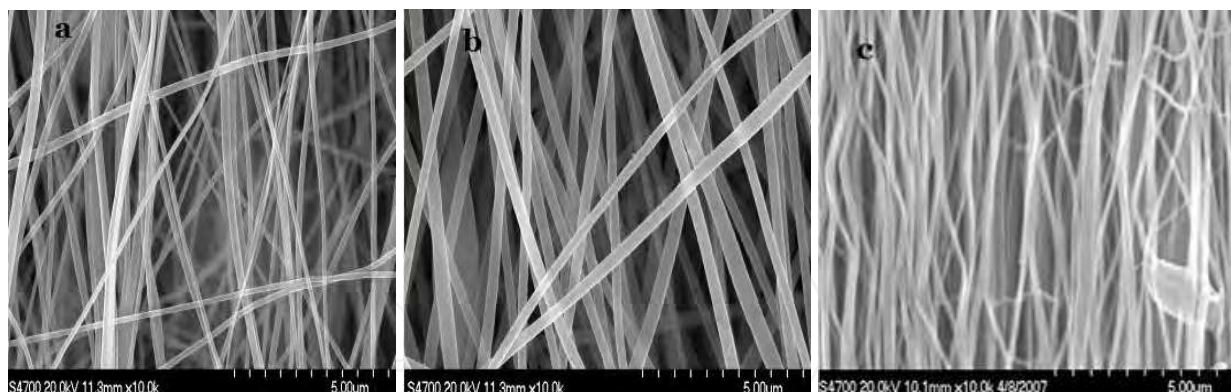


Fig. 10. SEM micrographs: (a) as-spun pure partially aligned PAN nanofibers; (b) PAN/SWNTs composite nanofibers with SWNTs concentration 1 wt%; (c) hot-stretched pure PAN nanofibers.

surface morphology of PAN nanofibers is smooth (Fig. 11(a)), but that of the PAN/SWNTs nanofibers is much rougher (Fig. 11(b)). Since the SWNTs possess a high electron density compared with the PAN polymer matrix, SWNTs appear as darker tubular structures embedded in the PAN/SWNTs composite nanofibers. It can be seen that the SWNTs are completely wrapped by the PAN matrix. TEM images reveals that in some regions nanotubes oriented well along the fiber axis but the nanotube distribution (number and orientation of the tubes) within a fiber may vary quite significantly (Fig. 11(b) and 11(c)). The nanotube distribution within a given fiber is usually quite different from the distribution in others. Topological defects such as entanglements, twisted sections, and knots can at times be observed (Fig. 11(d)). It is plausible that the extremely fast electrospinning process, by which carbon nanotubes cannot fully stretch within a millisecond range, leads to such defects.

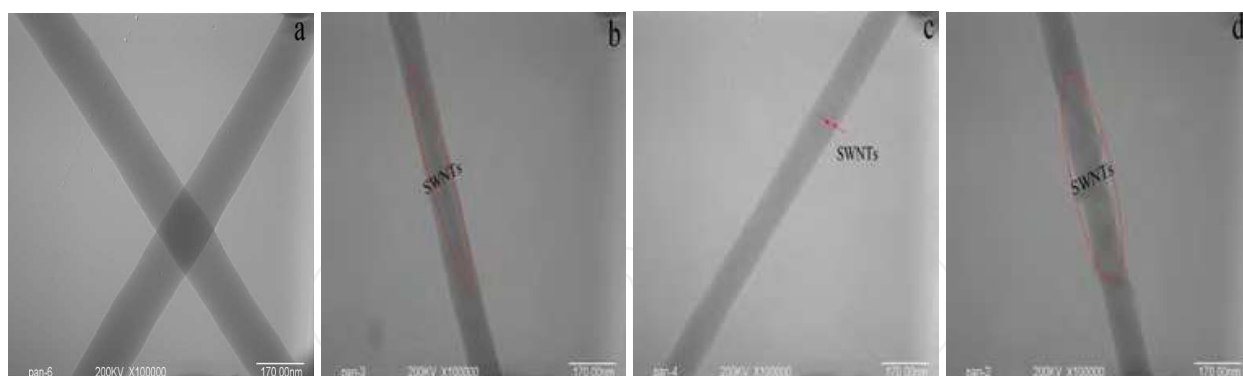


Fig. 11. TEM images: (a) PAN nanofibers; (b–d) PAN/SWNTs nanofibers with SWNTs concentration 1 wt%.

### 2.2.2 The alignment or the orientation of the as-spun, hot-stretched PAN and PAN-based nanofibers

The key determining the properties of the carbon fiber is the orientation of the polymer chain in the precursors. Usually the high degree of preferential orientation along the fiber axis of the layer planes is mainly responsible for the extraordinarily high Young's modulus of the fibers. Researchers now realize that understanding and controlling the orientation structure during the precursor formation step is critical if the properties of the carbon fibers

are to be optimized (Ruland 1990). Therefore, the research on the microstructure of the precursors under different processing conditions is important in the study of the final mechanical properties of the carbon fibers (Ko et al. 1989). However, due to the complicated process in the manufacture of carbon fibers, it is not easy and fast to determine the orientation factor for PAN precursors, especially the less theoretical studies on PAN precursors.

There are several methods to determine the alignment or orientation of the fibers, which are polarizing microscope, infrared dichroism, sound velocity method, X-ray diffraction (XRD) and pole figures etc. (Xu et al. 2005). For electrospinning nanofibers, since these are not really fibers from macroscopic point of view, usually only infrared dichroism, X-ray diffraction (XRD) and pole figures are suitable. Fig. 12(A), (B) and (C) show the XRD patterns from the as-spun and hot-stretched PAN nanofibers, and the pole figures of the electrospun PAN nanofibers as-spun and hot-stretched nanofibers respectively. The operation conditions are the 40 kV and 200 mA with produce CuK $\alpha$  radiation ( $\lambda = 1.54 \text{ \AA}$ ). There are two diffraction peaks at  $17^\circ$  and  $29^\circ$  which are corresponding to the  $d \approx 5.3 \text{ \AA}$  from the (100) and the  $d \approx 3.03 \text{ \AA}$  from the (110) reflections (Ra et al. 2005). The ratio of the  $d$ -spacing calculated by Bragg equation of these two peaks (1.74) is very close to  $\sqrt{3}:1$ , indicating hexagonal packing of the rod-like PAN chains (Zussman et al. 2005). The diffraction pattern of the as-spun nanofiber show one weak peak with a value of  $2\theta$  at  $17^\circ$ . And it also can be found that the peak at  $2\theta = 29.5^\circ$  became much bigger after the process of hot-stretched. This indicates that electrospinning of the nanofibers onto a rotating drum generates limited crystallinity. In contrast, the oriented nanofibers after hot-stretching also show two diffraction peaks indexed with values of  $2\theta$  of  $17^\circ$  and  $29^\circ$ . From Fig. 13(A), noted that the X-ray beam is directed perpendicular to normal of the nanofibers, and thus the beam is also parallel to the winding direction of the nanofibers. The pole figures also show the same results with the elliptical shape after hot-stretching. It means the nanofibers are highly oriented along the winding direction of the rotating drum collector. The orientation coefficient after hot-stretching increased about 21.5% in comparison with those of as-spun nanofiber.

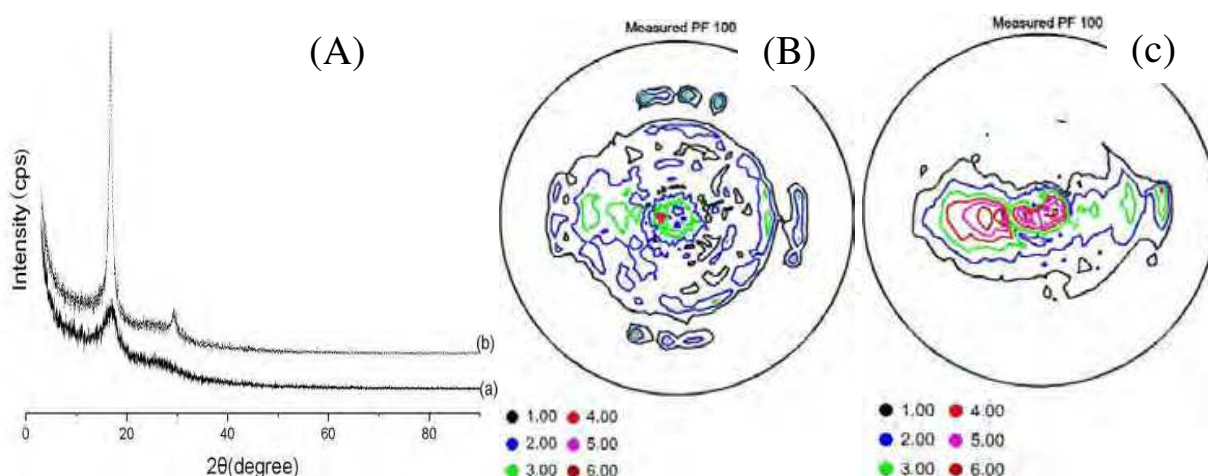


Fig. 12. (A) X-ray diffraction patterns for the nanofibers: (a) as-spun; (b) hot-stretched and the pole figures of the electrospun PAN nanofibers (B) as-spun nanofibers and (C) hot-stretched nanofibers.

The degree of orientation is usually expressed by orientation coefficient, which can be calculated from the half-width of the corresponding peak in the XRD curve. And the

Herman’s orientation factor,  $f$ , can be determined from the fully corrected azimuthal intensity distribution diffracted from the (100) reflection at  $d \approx 5.30 \text{ \AA}$  by equation (1).

$$f = \frac{\int_0^{90} \frac{(3 \cos^2 \varphi - 1)}{2} I \sin \varphi d\varphi}{\int_0^{90} I \sin \varphi d\varphi} \tag{1}$$

Where,  $\varphi$  is the azimuthal angle between the axis of the molecular segment and the fiber alignment, and  $I$  is the scattering intensity of the (100) reflection at that angle(Fennessey & Farris 2004). The orientation factor  $f$ , which can be calculated from equation (1), increased from 0.22 to 0.76 after the hot-stretched process correspondingly.

The electrospun fiber bundles can be examined using the infrared spectrometer (FTIR) with a polarized wire-grid to measure the dichroism of the nitrile-stretching (-CN) group vibration at  $2240 \text{ cm}^{-1}$  (Bashir et al. 1994). Spectra are acquired with the draw direction of the electrospun fibers positioned both parallel and perpendicular to the electric vector direction of the polarizer, which the results before and after hot-stretching show in Fig. 13. The spectra are recorded over the range of  $700\text{--}4000 \text{ cm}^{-1}$  with typically 64 scans. The dichroic ratio,  $D$ , and the chain orientation factor,  $f$ , can be calculated from Eqs. (2), (3) and (4) using the transition moment angle  $\alpha$  of  $70^\circ$  (or  $73^\circ$ ), which  $\alpha$  is the angle between the direction of the nitrile group's dipole moment change and the chain axis.

$$D = A_{//} / A_{\perp} \tag{2}$$

$$D_0 = 2 \cot^2 \alpha \tag{3}$$

$$f = \frac{(D - 1)(D_0 + 1)}{(D_0 - 1)(D + 2)} \tag{4}$$

where  $A_{//}$  is the absorbance when the electric vector direction of the polarizer is oriented parallel to the fiber draw direction and  $A_{\perp}$  is the absorbance when the electric vector is oriented perpendicular to the fiber draw direction,  $D_0$  is the dichroic ratio of an ideally oriented polymer,  $\alpha$  is the transition moment angle.

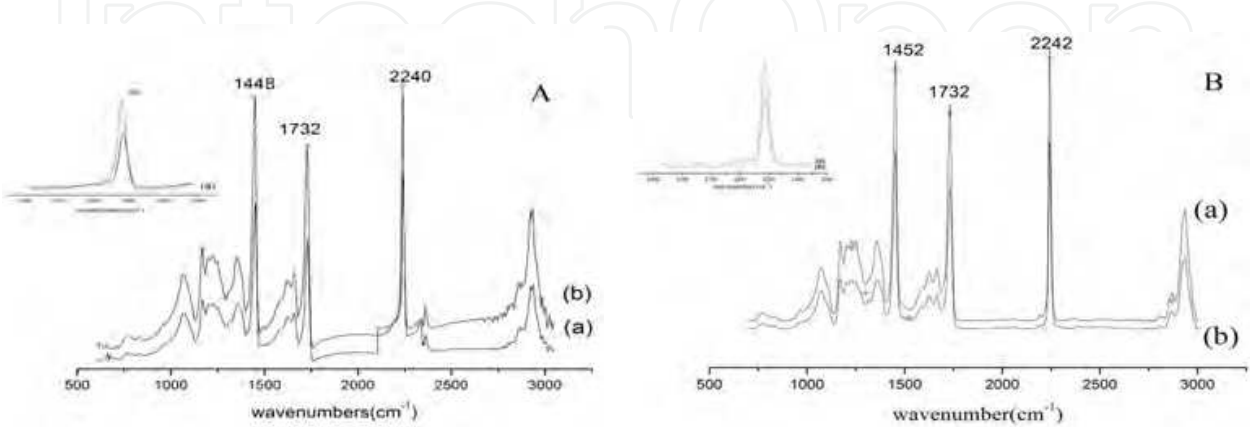


Fig. 13. Polarized FTIR spectra of PAN nanofiber: (A) before and (B) after hot-stretching, absorbent spectra at the perpendicular (a) and parallel (b) directions respectively.



In Fig. 13, the 2240 or 2242cm<sup>-1</sup> is the characteristic peak of PAN corresponding with the stretching vibration of -C≡N group, and the 1732cm<sup>-1</sup>, 1448 or 1452cm<sup>-1</sup> are the stretching vibration of C=O and bending vibration of C-H. It shows that no much change of the microstructure by hot-stretching process. The chain orientation factor, *f*, calculated from Eq. (4) is 0.46 and 0.65 before and after hot-stretching respectively, which shows the hot-stretching can enhance the chain orientation by the applied stretching force.

2.2.3 Crystallinities of the as-spun and hot-stretched PAN and PAN-based nanofibers

The crystallinities of the as-spun and hot-stretched PAN nanofiber can be also investigated with X-ray diffractometer (XRD). The percent crystallinity can be obtained by extrapolation of the crystalline and amorphous parts of the diffraction pattern. The crystallite size is calculated by using the formula as following equation:

$$L_c = k\lambda / (\beta \cos \theta)$$

(5)

where *k* = 0.89, *λ* = 1.54 Å, *β* is the full width Half maximum (FWHM), and *θ* is Bragg angle (Norman et al. 1998).

Table 1 presents values of the percent crystallinity and the orientation coefficient for these two types of nanofibers. The percent crystallinity of the hot-stretched nanofiber increased about 3-times in comparison with those of as-spun nanofiber. The crystallite size also increased about 162%, indicating highly oriented PAN nanofibers, which was in agreement with the results of the orientation factor. Fibers with larger PAN crystals and higher polymer molecular orientation are expected to lead to a more perfect and higher orientation carbon fiber with improved mechanical properties (Chae et al. 2005).

Nanofiber	Crystallinity (%)	Crystallite size(nm)
As-spun	11.27	4.14
Hot-stretched	38.34	10.83

Table 1. Percent crystallinity and crystallite size obtained from X-ray diffraction curves.

The *T<sub>g</sub>* of the PAN nanofiber and PAN/SWNTs nanofiber can be examined using Differential scanning calorimetry (DSC) method. To obtain the DSC curve in Fig. 14, the samples can be heated at a scanning rate of 20 °C/min under nitrogen atmosphere in order to diminish oxidation. The value of *T<sub>g</sub>* is found by differentiating the heat flow curve with the temperature.

Fig. 14(A) shows the DSC curves to determine the glass transition temperature (*T<sub>g</sub>*) of PAN and PAN/SWNTs nanofibers. It can be seen that, compares with PAN nanofiber (*T<sub>g</sub>* = 102.3°C), the *T<sub>g</sub>* is increased by about 3°C by incorporating only 0.75 wt% SWNTs into the PAN matrix (*T<sub>g</sub>* = 105.4°C). Increase in the glass transition temperature as compared to the PAN fiber provides the evidence of interaction between PAN and SWNTs. The improvement in the *T<sub>g</sub>* stemmed from a stronger interfacial interaction and possible covalent bonding between PAN and the SWNTs. Fig. 14(B) shows the DSC thermograms which the peak of PAN/SWNTs is higher than the one of PAN nanofibers. All these results suggests that the mobility of PAN chains is reduced due to the constraint effect of SWNTs (Chou et al. 2008).

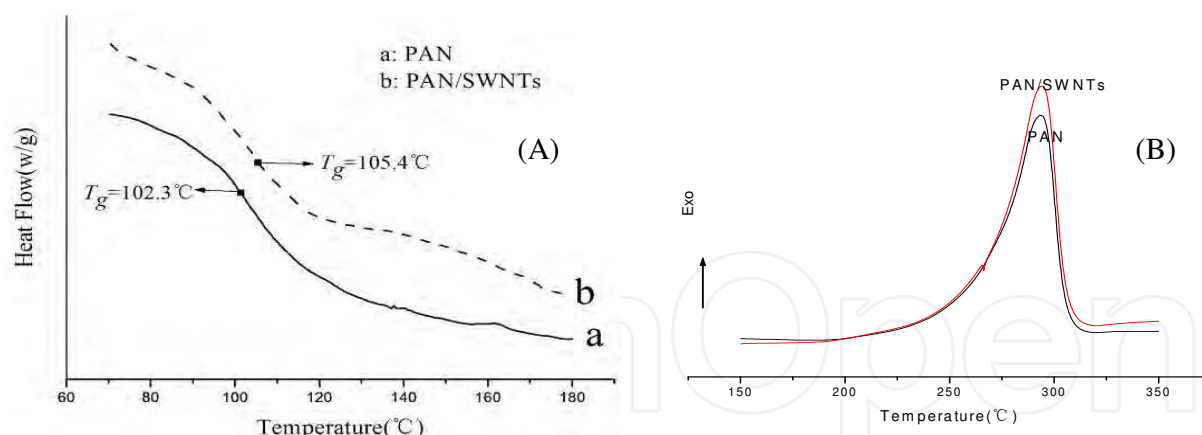


Fig. 14. (A)  $T_g$  from DSC of electrospun nanofibers: (a) PAN nanofibers; (b) PAN/SWNTs composite nanofibers; (B) DSC thermograms of electrospun PAN and PAN/SWNTs nanofibers.

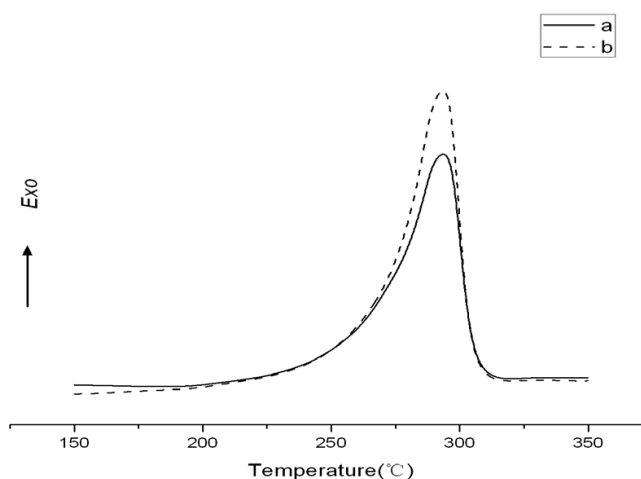


Fig. 15. DSC thermograms of PAN nanofiber sheets (a) before and (b) after hot-stretched.

Fig. 15 showed the DSC thermograms of PAN nanofiber sheets before and after hot-stretched process respectively. It can be seen that after hot-stretching, the peak and the peak area all increased. It means the cyclization heat of reaction enhances (from 510.53 J/g to 530.42 J/g) and the degree of cyclization increases correspondingly which is better for the manufacturing of the final carbon fibers.

## 2.2.4 Pre-oxidation treatment

The material, the process and the conditions used to form the precursor fiber, are the critical factors that define the final properties of the carbon fibers. Post-treatment steps such as pre-oxidation, stabilization and carbonization merely refine the as-spun structure (Paiva et al. 2001). The fundamental fiber structure needs to develop high properties must be created during the initial fiber formation step. However, this is not to say that fiber properties cannot be dramatically altered during the post-treatment (Edie 1998).

As infrared spectroscopy in Fig. 16(A) shows, with the pre-oxidation temperature increasing,  $-C\equiv N$  characteristic absorption band at  $2,243\text{ cm}^{-1}$  is decreasing. And the absorption peaks of  $-C=N-$  band characteristics at  $1,591\text{ cm}^{-1}$  and  $C-H$  features in the

band at  $1,371\text{ cm}^{-1}$  increase significantly with the increasing pre-oxidation temperature, which indicates that cyclization and dehydrogenation reaction has occurred in the pre-oxidation process of PAN nanofibers [9]. A new peak appears in the band at  $810\text{ cm}^{-1}$ . It indicates that  $\text{-C}=\text{C-}$  has come into being in the molecules during pre-oxidation process, which shows that aromatic structure and heat-resistant structure have formed. Fig. 16(B) shows the XRD curves under different pre-oxidization temperatures. It has been known that two diffraction peaks indexed with values of  $2\theta$  of  $17^\circ$  and  $29^\circ$  are corresponding with the (100) and (101) crystal planes. With the pre-oxidation temperature increased to  $230^\circ\text{C}$ , there is a new diffraction peak at  $25.2^\circ$  which is corresponding to the characteristic cyclization and aromatization structures of the (002) planes in graphite. It presented the dehydrogenation process in manufacturing of carbon fibers and the structure of linear PAN chain began to form the ladder structures which are corresponding to the decrease of the  $\text{-C}\equiv\text{N}$  characteristic peaks at  $2\theta$  of  $17^\circ$  and  $29^\circ$  and increase of the aromatization diffraction peak at  $25.2^\circ$ .

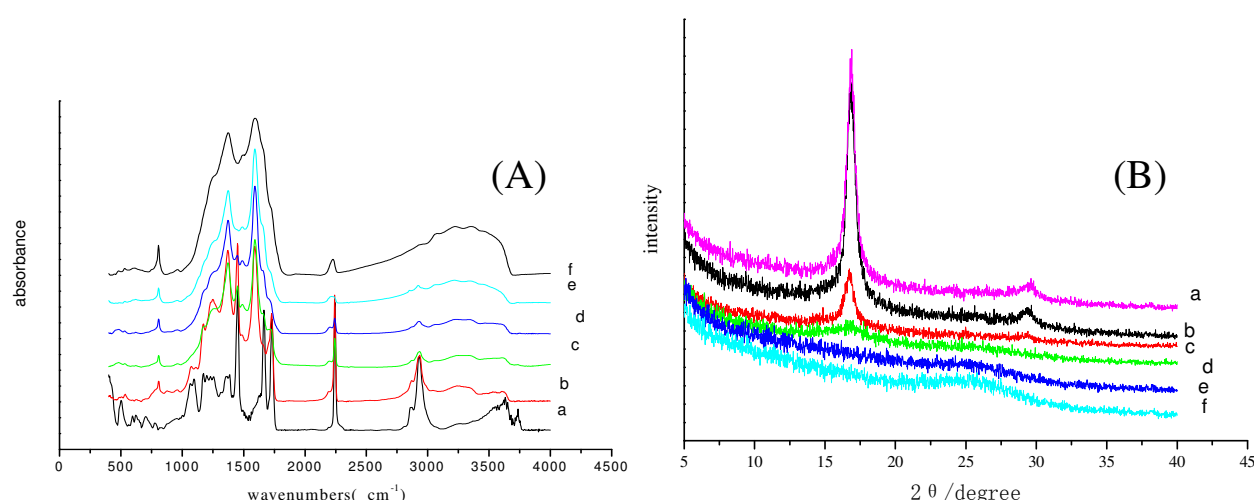


Fig. 16. (A) Infrared spectroscopy and (B) XRD curves under different pre-oxidization temperatures (a)  $135^\circ\text{C}$  (b)  $210^\circ\text{C}$  (c)  $230^\circ\text{C}$  (d)  $250^\circ\text{C}$  (e)  $270^\circ\text{C}$  (f)  $290^\circ\text{C}$ .

The aromatization index (AI) can be calculated with the following equation (Koganemaru et al. 2004):

$$AI = I_c / (I_c + I_p) \quad (6)$$

where  $I_p$  and  $I_c$  are the intensity of PAN at  $17^\circ$  and aromatization structure at  $25.2^\circ$  respectively. It can be calculated that the extent of aromatization increasing from 21.86% to 41.98% at pre-oxidation temperatures of 230 and  $270^\circ\text{C}$  respectively. And if the temperature increased to  $270^\circ\text{C}$ , the characteristic diffraction peak of  $\text{-C}\equiv\text{N}$  at  $17^\circ$  disappeared completely, which means that the higher pre-oxidation temperature is good for aromatization reaction.

### 2.2.5 Mechanical properties and electrical conductivities

A better representation of the nanocomposites characteristics is attempted by measuring the macroscopic nanofiber sheets. Stretching a piece of the nanofiber sheet gives an assessment of the average mechanical properties of the nanofibers rather than measuring an individual

segment of a nanofiber composite (Moniruzzaman & Winey 2006). Mechanical property testing can be performed by the normal Instron tensile tests such as a LR30K Electromechanical Universal Testing Machine. The aligned nanofibers films taken down from the 16cm×12cm paper frame with the hollow of 16cm×4cm in Fig. 3 can be used for further tests which usually there are eight specimens used for each nanofiber sample in the tensile test. The samples can be cut into the size of 5mm width and 20mm length. The tensile speed in the mechanical test is selected as normal one such as 20 mm/min. The cross section areas of the samples are calculated via the weights of the samples and the densities of PAN and SWNTs.

The stress-strain curves of PAN nanofibers, before and after hot-stretched respectively, are presented in Fig. 17(A). Hot-stretched improved tensile strength and the modulus of PAN nanofibers. The tensile strength and tensile modulus increased by 55.32% and 156.48% respectively. Table 2 lists the tensile strength, tensile modulus, and elongation at break can be obtained from the stress-strain curves.

Sample	Tensile strength(MPa)	Impro.(%)	Tensile modulus(GPa)	Impro.(%)	Elongation at break(%)
As-spun	51.84		1.08		22.05
hot-stretched	80.52	55.32	2.77	156.48	11.61

Table 2. Mechanical properties of PAN nanofiber sheets.

It can be concluded that the hot-stretched method can improve the mechanical properties of PAN nanofibers. During the process of hot-stretched, the PAN molecular chain moves and arranges again along the fiber axis, the orientation and crystallinity are also improved. Therefore the mechanical properties of PAN nanofibers are improved due to the improvement of orientation and crystallinity. The improvement of crystallite size results in the elongation at break decreased obviously. The increased polymer orientation and crystal size point to the potential of PAN/SWNTs composite nanofibers as the precursor for the next generation carbon fiber. The stress-strain curves of PAN/SWNTs nanofibers, before and after being hot-stretched, are presented in Fig. 17(B). Hot-stretched also improves the tensile strength and the modulus of PAN/SWNTs nanofibers, which the tensile strength and tensile modulus increased by 54.70% and 125.40% respectively. It can be concluded that the hot-stretching can notably improve the mechanical properties of PAN/SWNTs nanofibers.

Fig. 18 shows the stress-strain curves of the PAN nanofibers and PAN/SWNTs nanofiber composites with different concentrations (hot-stretching). It shows that the SWNTs improves the modulus and tensile strength of the nanofiber. The tensile strength 128.76MPa of the nanocomposites at about 0.75% SWNTs by weight is increased with 58.9%. Also the tensile modulus shows a peak value of 4.62GPa with 66.8% improvement. The (e) curve in Fig. 18 deviates from the trend, which might be the non-uniform dispersion of SWNTs in high concentration. The significant improvement in strength and modulus is likely related to the good dispersion and orientation of SWNTs within the polymer matrix, and the strong interfacial adhesion due to the SWNTs surface modification (Chou et al. 2008). It can be concluded that both hot-stretching and the introduction of SWNTs can improve the mechanical properties of PAN-based nanofibers significantly.



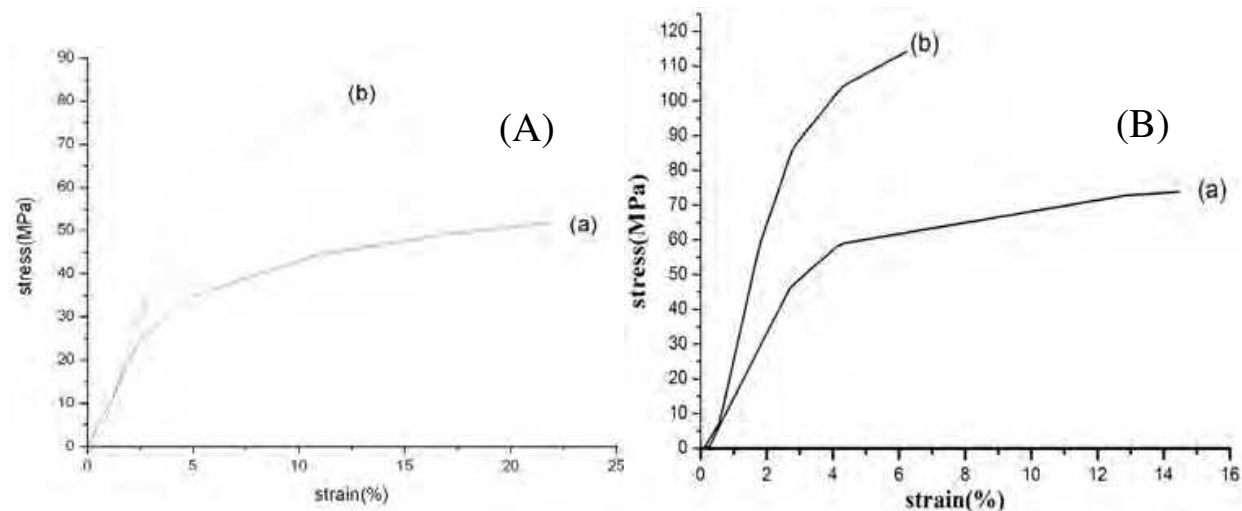


Fig. 17. Stress-strain curves of (A) PAN nanofiber sheets (a) before and (b) after hot-stretched and (B) PAN/SWNTs nanofiber sheets with SWNTs concentration 1 wt% (a) before and (b) after being hot-stretched.

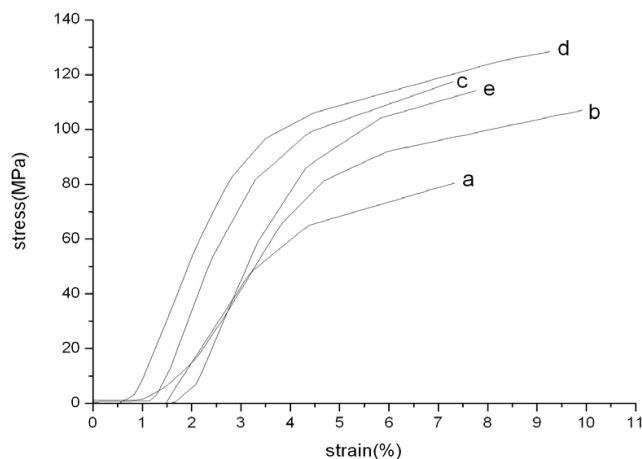


Fig. 18. Stress-strain curves for PAN and PAN/SWNTs Nanofiber: (a) pure PAN; (b) 0.25% SWNTs; (c) 0.5% SWNTs; (d) 0.75% SWNTs; (e) 1% SWNTs.

The electrical conductivities of electrospun PAN/SWNTs nanofiber composites can also be measured using the ultra-high resistance measuring machine at room temperature and ambient condition. The electrical conductivities can be obtained according to the formula as following:

$$\rho_v = R_v \times \frac{21.23}{t} \tag{7}$$

where  $\rho_v$  is volume resistivity,  $R_v$  is resistance, and  $t$  is the thickness of the nanofiber films. The electrical conductivity of the pure PAN nanofiber is 0.2-0.5 S/cm (Ge et al. 2004). Due to the superb electrical properties of SWNTs, a better electrical conductivity in PAN/SWNTs nanofiber composites is expected. Since electrical conductivity requires a percolating network be formed by the SWNTs, it can be concluded that the composite nanofibers, at a concentration of 0.75wt.% SWNTs, has formed the percolating network so that the

PAN/SWNTs nanofiber composites could possess electrical conductivity of up to 2.5 S/cm. Therefore these conductive PAN/SWNTs nanofiber sheets have potential applications in conductive nanoelectrodes, supercapacitors and nanosensors etc.

### 3. Conclusions

PAN nanofibers and PAN/SWNTs nanofiber composites can be prepared by electrospinning from PAN-based solution. An additional centrifugal field applied to an electrostatic field can produce a strong stretching force in electrospinning processes. Hot-stretched method and the incorporated CNTs are the key processes used to increase the degree of crystallinity and molecular orientation of PAN nanofibers and PAN/SWNTs nanofiber composites. The strong hot-stretching force can change the molecular orientation and an addition of only 0.75 wt% SWNTs to PAN increases the polymer mechanical properties significantly. SEM and TEM results show that SWNTs has a high orientation in PAN/SWNTs composite nanofibers. The crystallinity of the stretched sheet confirmed by X-ray diffraction has enhanced about 3 times in comparison with those of as-spun sheets and the chain orientation factor,  $f$ , is 0.46 and 0.65 before and after hot-stretching respective. Compared to pure PAN nanofibers, tensile strength and Young's modulus of the hot-stretched nanofibers exhibit considerable improvement. Thus, the improvement of orientation and crystallinity, the better PAN nanofibers alignment, are all contributed to the obvious increases of mechanical properties of the nanofibers. Incorporation of SWNTs into the nanofibers also increases the electrical conductivity to 2.5 S/cm for PAN/0.75% SWNTs nanofiber composites. Such PAN-based composite nanofiber sheets represent an important step toward utilizing carbon nanotubes in materials to achieve remarkably enhanced physical properties. Thus, the composite nanofibers with the component of SWNTs and the hot-stretched process can be used as the potential precursor to produce high-performance carbon nanofibers. The mechanical properties of the PAN nanofibers and PAN/SWNTs composite nanofibers can be improved more by extensive studies of electrospinning and the hot-stretching conditions. Thus, this novel electrospinning technique creates aligned and molecularly oriented PAN and PAN-based nanofibers that can be used to prepare carbon nanofibers with superior mechanical properties.

### 4. Acknowledgment

The authors gratefully acknowledge the financial support sponsored by the NSF of China(50973007) and the Program for Changjiang Scholars and Innovative Research Team in University (PCSIRT IRT0807).

### 5. References

- Andrews, R.; Jacques, D.; Rao, A.M.; Rantell, T.; Derbyshire F.; Chen, Y.; Chen, J.; Haddon, R.C. (1999). Nanotube composite carbon fibers, *Appl. Phys. Lett.*, Vol.75, pp.1329-1331
- Bashir, Z.; Church, S.; and Waldron, D. (1994). Interaction of water and hydrated crystallization in water-plasticized polyacrylonitrile films, *Polymer*, Vol.35, pp.967-97

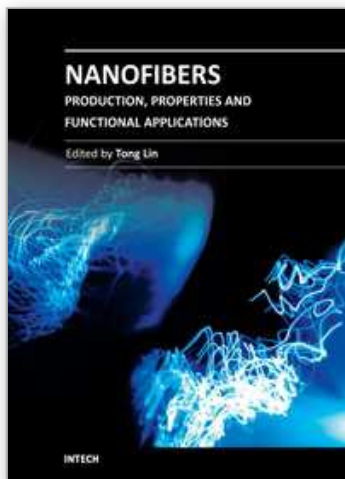
- Basova, Y.V.; Edie, D.D.; Lee, Y.S.; Reid, L.K. (2004). Effect of precursor composition on the activation of pitch-based carbon fibers, *Carbon*, Vol.42, pp.485–495
- Baughman, R.H.; Zakhidov, A.A.; de Heer, W.A. (2002). Carbon nanotubes-the route toward applications, *Science*, Vol.297, pp.787-792
- Chae, H.G.; Sreekumar, T.V.; Uchida, T; Kumar, S. (2005). A comparison of reinforcement efficiency of various types of carbon nanotubes in polyacrylonitrile fiber. *Polymer*, Vol.46, pp.10925-10935
- Chand, S. (2000). Carbon fibers for composites, *J. Mater. Sci.* Vol.35, pp.1303-1313
- Chandrasekar, R.; Zhang, L.F.; Howe, J.Y.; Hedin, N.E.; Zhang, Y.; Fong, H. (2009). Fabrication and characterization of electrospun titania nanofibers. *J. Mater. Sci.* Vol.44, pp.1198-1205
- Chen, J.; Ramasubramaniam, R.; Xue, C.; Liu, H. (2006). A versatile molecular engineering approach to simultaneously enhanced, multifunctional carbon-nanotube-polymer composites. *Adv. Funct. Mater.*, Vol.16, pp.114-119
- Chou, W.J.; Wang, C.C.; Chen, C.Y. (2008). Characteristics of polyimide-based nanocomposites containing plasma-modified multi-walled carbon nanotubes. *Compos. Sci. Technol.*, Vol.68, pp.2208-2213
- Chun, I.; Reneker, D.H.; Fong, H.; Fang, X.; Deitzel, J.; Beck-Tan, N. (1999). Carbon nanofibers from polyacrylonitrile and mesophase pitch. *J. Adv. Mater.*, Vol.31, No.1, pp.36–41
- Collins, P.G.; Arnold, M.S.; Avouris, Ph. (2001). Engineering carbon nanotubes and nanotube circuits using electrical breakdown, *Science*, Vol.292, pp.706.-709
- Donnet, J.B.; Wang, T.K.; Peng, J.C.; Rebouillat, S. (1998). Carbon fibers. New York, NY: Marcel Dekker; pp.231-309
- Doshi, J.; Reneker, D. H. (1995). Electrospinning process and applications of electrospun fibers, *J. Electrostat.*, Vol.35, pp.151–160
- Dzenis, Y. (2004). Spinning continuous fibers for nanotechnology, *Science*, Vol.304(5679), pp.1917–9
- Edie, D. D. (1998). The effect of processing on the structure and properties of carbon fibers, *Carbon*, Vol.36, pp.345–362.
- Fennessey, S.F.; Farris, R.J. (2004). Fabrication of aligned and molecularly oriented electrospun polyacrylonitrile nanofibers and the mechanical behavior of their twisted yarns. *Polymer*, Vol.45, pp.4217-4225
- Ge, J.J.; Hou, H.Q.; Li, Q.; Graham, M.J.; Greiner, A.; Reneker, D.H.; Harris, F.W.; and Cheng, S.Z.D. (2004). Assembly of Well-Aligned Multiwalled Carbon Nanotubes in Confined Polyacrylonitrile Environments: Electrospun Composite Nanofiber Sheets, *J. AM. CHEM. SOC.*, Vol.126, pp.15754-15761
- Hammel, E.; Tang, X.; Trampert, M.; Schmitt T.; Mauthner, K.; Eder, A. and Pötschke, P. (2004). Carbon nanofibers for composite applications, *Carbon*, Vol.42, pp.1153–1158
- Hao, R.; Yuan, J.Y.; Peng, Q. (2006). Fabrication and sensing behavior of Cr<sub>2</sub>O<sub>3</sub> nanofibers via in situ gelation and electrospinning. *Chem. Lett.*, Vol.35, pp.1248-1249
- Huang, Z.M.; Zhang, Y.Z.; Kotaki, M.; Ramakrishna, S. (2003). A review on polymer nanofibers by electrospinning and their applications in nanocomposites. *Compos. Sci. Technol.*, Vol.63, pp.2223-2253
- Iijima, S. (1991). Helical microtubules of graphitic carbon, *Nature*, Vol.354, pp.56-58

- Javey, A.; Guo, J.; Wang, Q.; Lundstrom, M.; Dai, H.J. (2003). Ballistic carbon nanotube field-effect transistors. *Nature*, Vol.424, pp.654-657
- Johnson, J.; Phillips L.N. and Watt, W. (1965). The production of carbon fibers. *British Patent*, 1,110,790
- Johnson, J.; Watt, W.; Phillips, L.N.; and Moreton, R. (1966). Improvements in or relating to carbonisable fibre and carbon fibre and their production. *British Patent*, 1,166,251
- Ko, T.H.; Lin, C.H.; Ting, H.Y. (1989). Structure changes and molecular motion of polyacrylonitrile fibers during pyrolysis. *J. Appl. Sci.*, Vol.37, pp.553-556
- Koganemaru, A.; Bin Y.Z.; Matsuo, M. (2004). Composites of Polyacrylonitrile and Mutiwallled Carbon Nanotubes Prepared by Gelation/Crystallization from solution. *Adv. Funct. Mater.*, Vol.14, pp. 842-850
- Li, D.; Wang, Y.; and Xia, Y. (2003). Electrospinning of polymeric and ceramic nanofibers as uniaxially aligned arrays, *Nano Letts*, Vol. 3, pp.1167-1171
- MacDiarmid, A., Jones, W., Norris, I., Gao, J., Johson, A., (2001). Electrostatically-generated nanofibers of electronic polymers, *Synthetic Metals*, Vol.119, 27-30
- Miaudet, P.; Bartholome, C.; Derre, A.; Maugey, M.; Sigaud, G.; Zakri, C.; Poulin, P. (2007). Thermo-electrical properties of PVA-nanotube composite fibers. *Polymer*, Vol.48, pp.4068-4074
- Moniruzzaman, M.; Winey, K.I. (2006). Polymer nanocomposites containing carbon nanotubes. *Macromolecules*, Vol.39, pp.5194-5205
- Morgan, P.E. (2005). Carbon fibers and their composites. Boca Raton, FL: CRC Press; pp. 185-267
- Na, H.; Li, Q.Y.; Sun, H.; Zhao, C.; Yuan, X.Y. (2009). Anisotropic mechanical properties of hot-pressed pvdf membranes with higher fiber alignments via electrospinning. *Polym. Eng. Sci.*, Vol.49, pp.1291-1298
- Norman, W.H.; Cheetham, W.H.; Tao, L.P. (1998). Variation in crystalline type with amylose content in maize starch granules: An X-ray powder diffraction study. *Carbohydr. Polym.*, Vol.36, pp.277-284
- Paiva, M.C.; Bernardo, C.A.; Edie, D.D. (2001). A comparative analysis of alternative models to predict the tensile strength of untreated and surface oxidized carbon fibers. *Carbon*, Vol.39, pp.1091-1101
- Ra, E.J.; An, K.H.; Kim, K.K.; Jeong, S.Y.; Lee, Y.H. (2005). Anisotropic electrical conductivity of MWCNT/PAN nanofiber paper. *Chem. Phys. Lett.*, Vol.413, pp.188-19
- Reneker D.H.; Chun, I. (1996). Nanometer diameter fibers of polymer, produced by electrospinning. *Nanotechnology*, Vol.7, No.3, pp.216-23
- Rilutsky, S.; Zussman, E.; Cohen Y. (2010). Carbonization of Electrospun Poly(acrylonitrile) Nanofibers Containing Multiwallled Carbon Nanotubes Observed by Transmission Electron Microscope with In Situ Heating, *Journal of Polymer Science: Part B: Polymer Physics*, Vol.48, pp.2121-2128
- Ruland W. (1990). Carbon-fibers. *Adv. Mater.*; Vol.2, pp.528-536
- Smalley, R.E.; Colbert, D.T.; Smith, K.A.; Michael, O. (2007). Polymer-wrapped single wall carbon nanotubes. *US Patent*, 201,001,437,18A
- Sreekumar, T.V.; Liu, T.; Min, B.G.; Guo, H.; Kumar S.; Hauge, R.H.; Smalley, R.E. (2004). Polyacrylonitrile single-walled carbon nanotube composite fibers, *Adv. Mater.*, Vol.16, pp.58-61



- Sutasinpromprae, J.; Jitjaicham, S.; Nithitanakul, M.; Meechaisue, C.; (2006). Supaphol, P. *Polym. Int.*, Vol.55, pp.825-833
- Taylor, G. (1969). Electrically Driven Jets,, *Proc. R. Soc. London, Ser. A*, Vol.313, pp.453-475
- Yu, M.F.; Lourie, O.; Dyer, M.J.; Moloni, K.; Kelly, T.F.; Ruoff, R.S. (2000). Strength and breaking mechanism of multi-walled carbon nanotubes under tensile load. *Science*, Vol.287, pp.637-640
- Waclawik, E.R.; John, B.J.; Goh, SGR; Anthony, M.; Nunzio, M. (2006). Self-organization in composites of poly(3-hexylthiophene) and single-walled carbon nanotubes designed for use in photovoltaic applications. *Proc. of SPIE*; Vol.6036, pp.603607-4.
- Wong, E.W.; Sheehan, P.E.; Lieber, C.M. (1997). Nanobeam mechanics: Elasticity, strength, and toughness of nanorods and nanotubes. *Science*, Vol.277, pp.1971-1975
- Xu, Q.; Xu, L.H.; Cao, W.Y.; and Wu S.Z. (2005). A study on the orientation structure and mechanical properties of polyacrylonitrile precursors. *Polym. Adv. Technol.*, Vol.16, pp.642-645
- Zussman, E.; Chen, X.; Ding, W.; Calabri, L.; Dikin, D.A.; Quintana, J.P.; Ruoff, R.S. (2005). Mechanical and structural characterization of electrospun PAN-derived carbon nanofibers. *Carbon*, Vol.43, pp.2175-2185

IntechOpen



## **Nanofibers - Production, Properties and Functional Applications**

Edited by Dr. Tong Lin

ISBN 978-953-307-420-7

Hard cover, 458 pages

**Publisher** InTech

**Published online** 14, November, 2011

**Published in print edition** November, 2011

As an important one-dimensional nanomaterial, nanofibers have extremely high specific surface area because of their small diameters, and nanofiber membranes are highly porous with excellent pore interconnectivity. These unique characteristics plus the functionalities from the materials themselves impart nanofibers with a number of novel properties for advanced applications. This book is a compilation of contributions made by experts who specialize in nanofibers. It provides an up-to-date coverage of in nanofiber preparation, properties and functional applications. I am deeply appreciative of all the authors and have no doubt that their contribution will be a useful resource for anyone associated with the discipline of nanofibers.

### **How to reference**

In order to correctly reference this scholarly work, feel free to copy and paste the following:

Chen Zhang, Xuejia Ding and Sizhu Wu (2011). The Microstructure Characterization and the Mechanical Properties of Electrospun Polyacrylonitrile-Based Nanofibers, *Nanofibers - Production, Properties and Functional Applications*, Dr. Tong Lin (Ed.), ISBN: 978-953-307-420-7, InTech, Available from: <http://www.intechopen.com/books/nanofibers-production-properties-and-functional-applications/the-microstructure-characterization-and-the-mechanical-properties-of-electrospun-polyacrylonitrile-b>

**INTECH**  
open science | open minds

### **InTech Europe**

University Campus STeP Ri  
Slavka Krautzeka 83/A  
51000 Rijeka, Croatia  
Phone: +385 (51) 770 447  
Fax: +385 (51) 686 166  
[www.intechopen.com](http://www.intechopen.com)

### **InTech China**

Unit 405, Office Block, Hotel Equatorial Shanghai  
No.65, Yan An Road (West), Shanghai, 200040, China  
中国上海市延安西路65号上海国际贵都大饭店办公楼405单元  
Phone: +86-21-62489820  
Fax: +86-21-62489821

© 2011 The Author(s). Licensee IntechOpen. This is an open access article distributed under the terms of the [Creative Commons Attribution 3.0 License](https://creativecommons.org/licenses/by/3.0/), which permits unrestricted use, distribution, and reproduction in any medium, provided the original work is properly cited.

IntechOpen

IntechOpen